

Contraction-based Variations in Upper Limb EMG-Force Models under Isometric Conditions

Katherine Mountjoy
 Department of Electrical and
 Computer Engineering
 Queen's University
 Kingston, ON
 Email: 6kcm@queensu.ca

Evelyn Morin
 Department of Electrical and
 Computer Engineering
 Queen's University
 Kingston, ON
 Email: morine@post.queensu.ca

Keyvan Hashtrudi-Zaad
 Department of Electrical and
 Computer Engineering
 Queen's University
 Kingston, ON
 Email: khz@post.queensu.ca

Abstract—In this work, a previously developed model, which maps joint kinematic data and estimated muscle activation levels to net elbow joint torque, is trained with 4 groups of datasets in order to improve force estimation accuracy and gain insight into muscle behaviour. The training datasets are defined such that surface electromyogram (EMG) and force data are grouped within individual trials, across trials, within force levels and across force levels, and model performance is assessed. Average evaluation error ranged between 5% and 15%, with the lowest error observed for models trained with datasets grouped within separate force levels. Model error is further reduced when training datasets are grouped across data collection trials. Therefore, more accurate estimation of elbow joint behaviour can be accomplished by taking into account the functional requirements of muscle, and allowing for separate models to be developed accordingly.

I. INTRODUCTION

The force generated by a muscle depends on muscle activation dynamics - the excitation signal and motor unit recruitment in muscle, and muscle contraction dynamics - the mechanical properties of musculotendon units dictated by length and velocity relationships [1]. Muscle activation is defined as the neural input for a desired muscle force and is commonly estimated from recorded electromyogram (EMG). EMG amplitude is observed to increase when more force is generated in a muscle, however it has been noted that models describing the force produced in muscle do not scale linearly with muscle activation level [2], [3].

The magnitude of force generated by a particular muscle is modified by varying the number (recruitment) and frequency with which motor units are instructed to contract [4]. It has also been shown that the maximal force output of muscle shifts towards longer muscle lengths in submaximal contractions [5], [6], [7]. As the functional requirements of muscle change, so do the models that would be used to describe the joint dynamics. [8]

Many researchers have attempted to develop models to predict muscle force from an estimate of muscle activation based on measured EMG using non-linear identification methods such as neural networks [9] or polynomial fitting [10]. However, in general, these models do not reflect the nature of joint motion as they are not derived from a physiological

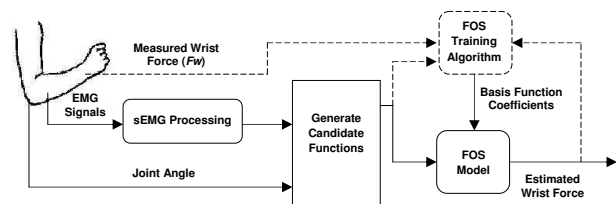


Fig. 1. Proposed force observer. Dashed lines represent signals used for training.

basis. In previous work, a physiologically-based model was developed using the Fast Orthogonal Search (FOS) method to map joint kinematic data and muscle activation level, estimated from surface EMG (sEMG), to net elbow torque (expressed as force at the wrist) under isometric conditions [11]. Good performance was achieved by this model, which gave estimation errors of 10% [11]. The aim of the research reported here is to tailor the training data to develop sEMG-Force models which achieve a better representation of upper limb muscle behaviour during submaximal isometric contractions at two output force levels, and thereby obtain better force estimation accuracy.

II. EMG FORCE MAPPING USING FAST ORTHOGONAL SEARCH

A. Fast Orthogonal Search (FOS)

Fast Orthogonal Search (FOS) is a nonlinear identification method that approximates a system output $y(n)$ with a weighted sum of M linear or nonlinear basis functions $p_m(n)$ and coefficient terms a_m and aims to minimize the mean square error between the estimate and $y(n)$ [12]. The FOS model takes the form:

$$y(n) = \sum_{m=1}^M a_m p_m(n) + e(n) \quad (1)$$

where a_m are coefficient terms, $e(n)$ is the estimation error and n is the discrete time sample index. The FOS method searches through a number, N , of available candidate basis functions, where $N \gg M$ and iteratively selects those functions which contribute the greatest reduction in mean

square error (MSE) between the model estimate and the actual system output. A detailed description of the method can be found in [13].

FOS models are generated using a designated *training set* as shown in Figure 1, and evaluated in a *leave-one-out* manner, where all datasets for the same data collection session with the exception of the training set are used to evaluate the model. Average estimation error was measured using percent relative mean square error (%RMSE):

$$\%RMSE = \frac{\sum_{i=1}^n (F_{wi} - \hat{F}_{wi})^2}{\sum_{i=1}^n F_{wi}^2} \times 100 \quad (2)$$

where F_{wi} is the measured force at the wrist and \hat{F}_{wi} is the FOS model estimate of wrist force.

Previous research [13] used a pool of FOS candidate functions composed of common mathematical terms, in order to develop FOS models which accurately predicted the force at the wrist during elbow flexion and extension. This method was further improved in [11] to better reflect the neuromuscular behaviour by incorporating Hill-based muscle model components into the pool of FOS candidate functions. Force estimation error averaged at 10%, however there remains room for improvement. The current work attempts to obtain more accurate force estimation results using Hill-based FOS models, by modifying the way in which FOS training sets are created. It is hoped that better FOS models will be developed for each subject by taking into account the differences in muscle behaviour at different activation levels.

B. Elbow Joint Dynamics and Hill-muscle Model Development

Elbow joint motion is a result of the contraction of elbow flexor muscles (the biceps brachii, brachioradialis and brachialis) and elbow extensors (triceps brachii and anconeus) to create smooth joint rotation. The moment generated by each muscle is a function of the muscle force and the muscle moment arm. The net moment about the elbow, M_{elbow} can be calculated as the sum of individual moments generated by each muscle, that is

$$M_{elbow} = \sum_{i=1}^I F_i \cdot MA_i = F_w \cdot MA_f \quad (3)$$

where i represents an individual muscle, I is the number of muscles acting on the joint, F_i is the force generated by muscle i , MA_i is the moment arm of muscle i , and the net moment about the elbow can be calculated from the force measured at the wrist F_w , using the length of the forearm as the moment arm MA_f . Using a Hill-muscle model [1], [14] that is composed of a contractile element (CE), a series elastic element (SE), and a parallel elastic element (PE) as shown in Figure 2, individual muscle forces can be estimated using the

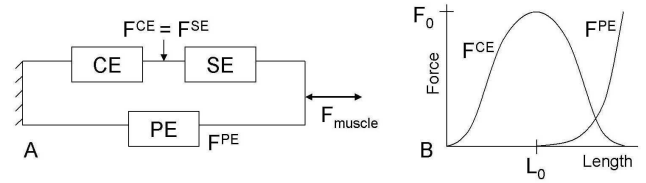


Fig. 2. A: Structure of the Hill muscle model adapted from [1]. B: Isometric contractile element force F^{CE} and parallel elastic element force F^{PE} as a function of muscle length. Note: the actual shape of F^{CE} is asymmetric.

following equations:

$$F^{CE} = F^{SE} \quad (4)$$

$$F_{muscle} = F^{CE} + F^{PE} \quad (5)$$

$$F^{CE} = F_0 \cdot f_l \cdot f_v \cdot a(t) \quad (6)$$

Here the contractile force generated by the CE (F^{CE}) can be interpreted as the activity of the contractile units within the muscle fibre and is equal to the force in the SE (F^{SE}) (4). The force generated by the PE component (F^{PE}) is attributed to the stretch resistance in inactive muscle. The PE only exerts tension when the muscle is stretched beyond L_0 . Tension builds up slowly at first, and then rapidly increases as shown in Figure 2. The total muscle force F_{muscle} equals the sum of the forces in each of the two parallel sections of the model (5). F^{CE} can be expressed as the product of F_0 , the force-length (f_l) and force-velocity (f_v) relationships, and muscle activation $a(t)$ [1] as in (6).

For an isometric contraction, the output F^{CE} peaks at F_0 at the optimal muscle length, L_0 , and for maximum muscle activation, and is reduced to zero at lengths of approximately $0.5L_0$ and $1.5L_0$ [1], as shown in Figure 2. In this study, the muscle length change contribution from the SE component was neglected [15]. During isometric contractions, the shortening velocity is zero and therefore f_v in (6) was set to 1.

The Hill-based model used in this study includes estimates for the F^{CE} and F^{PE} curves for the biceps brachii, brachioradialis and triceps brachii muscles. These functions were expressed in terms of joint angle rather than muscle length, due to the relative ease of measuring external elbow joint angle *in-vivo*. A relationship describing the change in muscle length for the elbow flexors and extensors with respect to elbow joint angle, presented by Lemay and Crago [16], was used to express F^{CE} and F^{PE} curves as a function of joint angle using a range of optimal joint angles spanning 20° - 120° in 10° intervals and using a constant term for muscle moment arm. The mapped F^{CE} and F^{PE} curves were then approximated using Gaussian functions and 2nd-order polynomials, respectively. Details of model generation are provided in [11].

C. Model Identification

The pool of N candidate functions (P), from which the FOS models are created, incorporates the Hill-based muscle model estimates for F^{CE} and F^{PE} into functions which represent

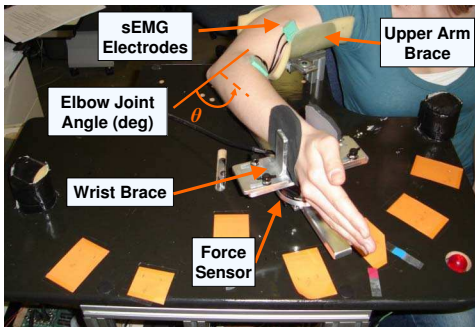


Fig. 3. Subject positioned in the QARM (1-DOF Queen's University Arm)

an expression of each muscle's contribution to isometric elbow moment at the wrist, that is

$$C = \begin{cases} F^{CE}(\theta_{0i}, \varphi_{vTi}) \cdot \frac{MA_i}{MA_f} = \frac{F_{0i} \cdot f_{li}(\theta_{0i}, \varphi_{vTi}) \cdot a_i(t) \cdot MA_i}{MA_f} \\ F^{PE}(\theta_{0i}) \cdot \frac{MA_i}{MA_f} = \frac{F^{PE}(\theta_{0i}) \cdot MA_i}{MA_f} \end{cases} \quad (7)$$

where i represents the specific muscle, and MA_f is constant for each subject as the measured length of the subject's forearm. Constant terms in the F^{CE} and F^{PE} equations, i.e. F_{0i} , MA_f and MA_i , were set equal to 1. This allows FOS to choose coefficient values which tailor the model to best reflect the physiology of the subject or the muscle activation level of the contraction.

The force-length component of the F^{CE} function depends on the value chosen for the optimal joint angle θ_{0i} in its equation as well as a parameter (φ_{vi}) which describes the shape of the Gaussian curve approximation. A total of 33 F^{CE} candidate functions were generated for each muscle, each reflecting one of 11 optimal joint angles ($20^\circ, 30^\circ, \dots, 120^\circ$) and one of three values for φ_{vi} as described in [11], resulting in a total of 99 functions included in the candidate pool. Similarly, 11 F^{PE} equations were generated for each muscle for the 11 values of θ_{0i} , resulting in a total of 33 F^{PE} functions included in the pool of candidates. Therefore, the entire candidate pool included a total of $N=132$ functions.

Models were generated for each subject with a pre-determined model size of 7 based on findings from Mobasser *et al.* [13]. The FOS method is structured such that the first function in the model is not chosen from the pool of candidates, rather it is assigned a value of 1, with a coefficient term to account for bias in the system. Subsequently, the function which contributes the greatest error reduction to the model is selected. This function is classified based on the muscle it represents and the value of θ_{0i} used in its calculations. From then on, the pool of candidate functions remaining for that muscle is limited to only those functions with the same $\theta_{0i} \pm 10^\circ$.

NC, WT	Set 1	Set 2	Set 3	Set 4	Set 5	Set 6	NC, AT	Set 1	Set 2	Set 3	Set 4	Set 5	Set 6
Trial 1	A	A	A	A	A	A	Trial 1	A	H	G	F	E	D
Trial 2	B	B	B	B	B	B	Trial 2	B	A	H	G	F	E
Trial 3	C	C	C	C	C	C	Trial 3	C	B	A	H	G	F
Trial 4	D	D	D	D	D	D	Trial 4	D	C	B	A	H	G
Trial 5	E	E	E	E	E	E	Trial 5	E	D	C	B	A	H
Trial 6	F	F	F	F	F	F	Trial 6	F	E	D	C	B	A
Trial 7	G	G	G	G	G	G	Trial 7	G	F	E	D	C	B
Trial 8	H	H	H	H	H	H	Trial 8	H	G	F	E	D	C

C, WT	Set 1	Set 2	Set 3	Set 4	Set 5	Set 6	C, AT	Set 1	Set 2	Set 3	Set 4	Set 5	Set 6
Trial 1	A	A	A	A	A	A	Trial 1	A	D	C	B	A	D
Trial 2	B	B	B	B	B	B	Trial 2	B	A	D	C	B	A
Trial 3	C	C	C	C	C	C	Trial 3	C	B	A	D	C	B
Trial 4	D	D	D	D	D	D	Trial 4	D	C	B	A	D	C
Trial 5	E	E	E	E	E	E	Trial 5	E	H	G	F	E	H
Trial 6	F	F	F	F	F	F	Trial 6	F	E	H	G	F	E
Trial 7	G	G	G	G	G	G	Trial 7	G	F	E	H	G	F
Trial 8	H	H	H	H	H	H	Trial 8	H	G	F	E	H	G

Fig. 4. Four groups of datasets used to train and evaluate FOS models

D. EMG Data Collection and Processing

III. EMG DATA COLLECTION AND PREPARATION

Experiments were conducted on a 1-Degree-of-freedom (DOF) exoskeleton testbed that holds the shoulder and wrist of each subject in a fixed position, and constrains flexion and extension of the right arm to the horizontal plane, as shown in Figure 3. A 6-DOF force/torque sensor was fixed to the wrist brace and used to measure linear force at the wrist. Details are described in [11].

Surface EMG data from the biceps brachii, brachioradialis and triceps brachii muscles were collected from the right arm of 10 subjects (4 male, 6 female) with a mean age of 25. Subjects had no known neuromuscular deficits of the right arm. The experimental protocol has been approved by the Health Sciences Research Ethics Board, Queen's University and subjects gave informed consent prior to participating in the study. Two Invenium Technologies active bipolar sEMG electrode units were placed adjacent to each other and secured over the belly of each of the three muscles. The sEMG data were processed using a linear envelope and normalized to a sustained 5Nm isometric contraction in both flexion and extension, as in [11].

Subjects performed a series of 12 isometric contractions (six in flexion and six in extension) at six joint angles ($30^\circ, 45^\circ, 60^\circ, 75^\circ, 90^\circ, \text{ and } 105^\circ$), taking full arm extension as an angle of 0° . This series of six contractions was classified as one *trial*. This procedure was repeated 8 times per data collection session. Visual wrist force feedback was provided to the subjects to aid in generating a desired wrist force. A target wrist force level of 10N was used in the first four trials and a target wrist force level of 20N for the remaining four trials in each session. Two minutes of rest was enforced between trials to prevent muscle fatigue. Data were collected in two or three separate sessions on different days.

A. Creation of FOS Model Training Sets

Previous Hill-based FOS models [11] were trained using one entire data record for 1 data collection trial, containing not only six contractions in flexion and extension, but also rest time between contractions and slight movements of the subjects' arms as they navigated from one test angle to another.

TABLE I
EVALUATION %RMSE FOR FOS MODELS GENERATED AND EVALUATED USING NC,WT DATASETS AND C,WT DATASETS CATEGORIZED FOR 10N AND 20N

Subject	Evaluation %RMSE (SD)		
	NC,WT	C,WT (10N)	C,WT (20N)
M1	14.8(10.7)	18.9(16.1)	6.1(2.8)
M2	9.4(5.0)	8.5(2.3)	4.4(1.3)
M3	7.0(3.6)	6.4(2.5)	4.2(2.3)
M4	36.0(22.5)	31.0(22.0)	15.9(9.4)
F1	9.0(4.5)	6.4(1.5)	4.7(1.4)
F2	11.5(7.5)	11.2(5.6)	5.8(3.3)
F3	37.0(28.4)	17.0(10.1)	8.8(3.9)
F4	9.7(6.0)	5.7(2.3)	4.0(1.1)
F5	5.8(3.3)	6.5(4.2)	3.6(1.5)
F6	8.5(5.8)	3.2(0.8)	3.6(1.0)
Average	14.9 (9.7)	11.5 (6.7)	6.1 (2.8)

TABLE II
EVALUATION %RMSE FOR FOS MODELS GENERATED AND EVALUATED USING NC,AT DATASETS AND C,AT DATASETS CATEGORIZED FOR 10N AND 20N

Subject	Evaluation %RMSE (SD)		
	NC,AT	C,AT (10N)	C,AT (20N)
M1	11.0(5.3)	8.5(3.6)	5.1(1.9)
M2	7.4(3.0)	8.6(2.4)	3.9(0.7)
M3	5.8(2.4)	6.5(2.2)	4.2(2.1)
M4	26.3(15.0)	26.8(13.8)	11.7(5.9)
F1	7.7(3.5)	6.2(1.3)	4.5(1.0)
F2	10.2(5.2)	10.0(3.5)	4.7(1.5)
F3	22.6(11.7)	14.1(5.0)	8.4(2.9)
F4	8.7(5.4)	5.1(1.3)	3.9(0.9)
F5	5.5(2.0)	6.1(2.6)	3.4(0.9)
F6	8.4(5.3)	3.2(0.5)	3.6(1.0)
Average	11.4 (5.9)	9.5 (3.6)	5.3 (1.9)

To create more successful FOS training sets, each trial of data for each subject containing six individual isometric contractions in flexion and extension was segmented into six distinct components, where each component or *set* included data for one active isometric contraction in flexion and extension. These contraction sets were then re-arranged in one of four ways to create new groups of FOS training sets.

Groups of datasets were either *categorized* (C) or *not-categorized* (NC) based on the output force level (10N or 20N). Within both C and NC groups, the extracted data segments were grouped *within trials* (WT) or *across trials* (AT) in a diagonal pattern. This resulted in four data groups - C,WT; C,AT; NC,WT; NC,AT - as shown in Figure 4, where the letters A-H associated with each contraction *set* and each *trial* indicate which data is included in each training set. In the C groups, the FOS models were trained and evaluated using datasets collected at the same output force level, whereas in the NC groups, the models were trained and evaluated using data collected at both force levels.

IV. FOS MODEL PERFORMANCE

FOS models were trained and evaluated using datasets grouped based on the C,WT; C,AT; NC,WT and NC,AT data groups previously described. This procedure was performed for each subject using data from either two or three data collection sessions.

The estimation error (%RMSE) associated with each model was calculated and averaged for all models within a data collection session for each subject to give a *mean* %RMSE ($RMSE_{AVE}$). These $RMSE_{AVE}$ values were then averaged again across all data collection sessions for one subject and are provided in Tables I and II. The success of the Hill-based FOS models to predict wrist force was consistent across subjects and sessions, with average $RMSE_{AVE}$ across all subjects ranging between 5-15% as shown in Tables I and II. Wilcoxon signed-rank tests for paired samples were performed to compare model performance using the four data grouping methods with a significance level set at ($p < 0.05$).

Evaluation %RMSE for all four data groups was the largest at 15% for models trained and evaluated with NC,WT datasets. Estimation error was improved with both data diagonalization (NC,AT) and with categorization (C,WT and C,AT).

Models trained using NC,WT were developed to model a series of isometric contractions at one output force level, however more than half of the evaluations were performed for datasets with contractions at a different muscle activation level. At 10N and 20N, the muscle has different functional behaviour. As a result, one model cannot provide a good approximation. Therefore, elbow muscles may be modeled for a variety of force levels or activities. Not surprisingly, a dramatic improvement in evaluation error (both the %RMSE and SD) was observed for C,WT(10N) and C,WT(20N) models when compared to the NC,WT models. Average $RMSE_{AVE}$ across all subjects dropped from 14.1% to 11.5% and 6.1% for the C,WT(10N) and C,WT(20N) models respectively. Paired comparisons were performed between the $RMSE_{AVE}$ for all subjects using NC,WT and for both C,WT(10N) and C,WT(20N) and a significant reduction in model error as well as a reduction in standard deviation was observed for both comparisons.

It is also interesting to note the reduction in model error and standard deviation between the C,WT(20N) and the C,WT(10N) models. A paired comparison confirmed that this reduction was statistically significant ($p < 0.05$). Explanation for this lower %RMSE can be attributed to a number of factors: The sEMG data contained in the 20N contractions is richer due to the increased recruitment and firing frequency of motor units in the upper-limb muscles for stronger contractions. It is likely that the subjects were better able to control the isometric contractions at 20N than 10N, resulting in more consistent data. As well, increased signal attenuation due to tissue filtering may have occurred for the 10N contractions, resulting in poorer quality sEMG signals.

An improvement in model estimation error and standard deviation was also observed between NC,WT and NC,AT

models. A paired comparison revealed that $RMSE_{AVE}$ for NC,AT (11.4%) was significantly lower than $RMSE_{AVE}$ for NC,WT (14.9%). It is assumed that using the diagonalized pattern of arranging individual contraction sets ensured that each training set contained data from multiple trials, thus addressing issues with inter-trial variability, as well as including contractions for both the 10N and 20N contraction level.

Finally, the best model performance was observed for models generated using C,AT(10N) and C,AT(20N) datasets. $RMSE_{AVE}$ was significantly lower for these two groupings at 9.5% and 5.3% respectively, than the $RMSE_{AVE}$ found for NC,AT (11.4%). As well, the standard deviations reported for C,AT(10N) and C,AT(20N) are half of the values reported for C,WT(10N) and C,WT(20N) and NC,AT models. To further assess the validity of using segmented datasets, A paired comparison between the C,WT(10N) and C,AT(10N) as well as between the C,WT(20N) and C,AT(20N) models revealed a significantly lower error for the segmented models ($p < 0.05$).

It appears that training FOS models using datasets that have been arranged in a segmented pattern across multiple data collection trials will produce models that are more accurate for individual subjects. In addition, developing separate models based on functional requirements of muscle (i.e. for specific force output levels) also results in more accurate estimation of elbow joint behaviour.

V. CONCLUSIONS

The goal of this research was to build upon previous work [11], [13] using Fast Orthogonal Search, to obtain more accurate estimates of isometric elbow joint torque expressed as force at the wrist. Four methods of grouping the contraction data were compared. The most dramatic improvements in model evaluation error were observed when models were trained and evaluated using datasets with similar muscle output force levels; however, significant improvements were also observed for models containing contraction data arranged in a segmented pattern across multiple trials. Since models of muscle properties have shown that force does not scale linearly with muscle activation level, separating the FOS models by target contraction force better represents the muscle behaviour at various submaximal activation levels.

Expanding on the utility of this method will require a larger data pool containing isometric contractions that excite additional activation levels. In addition, narrowing the resolution of optimal joint angles used in the Hill-based model identification from 10° to 5° may offer further reductions in model estimation error.

VI. ACKNOWLEDGMENTS

The authors wish to thank the volunteer subjects for their help and patience.

REFERENCES

[1] F. E. Zajac, "Muscle and tendon: properties, models, scaling and application to biomechanics and motor control," *Crit. Rev. Biomed. Eng.*, vol. 17, pp. 359–411, 1989.

[2] I. E. Brown, E. J. Cheng, and G. E. Loeb, "Measured and modeled properties of mammalian skeletal muscle. ii. the effects of stimulus frequency on force-length and force-velocity relationships," *J. Muscle Res. Cell Motil.*, vol. 20, pp. 627–643, 1999.

[3] M. Solomonow, R. Baratta, B. H. Zhou, H. Shoji, and R. D. D'Ambrosia, "The emg-force model of electrically stimulated muscle: Dependence on control strategy and predominant fiber composition," *IEEE Trans. Biomed. Eng.*, vol. 34, pp. 692–703, 1987.

[4] C. J. De Luca, "The use of surface electromyography in biomechanics," *J. Appl. Biomech.*, vol. 13, pp. 135–163, 1997.

[5] J. S. Leedham and J. J. Dowling, "Force-length, torque-angle and emg-joint angle relationships of the human in vivo biceps brachii," *Eur. J. Appl. Physiol.*, vol. 70, pp. 421–426, 1995.

[6] E. A. Hansen, H. D. Lee, K. Barrett, and W. Herzog, "The shape of the force-elbow angle relationship for maximal voluntary contractions and sub-maximal electrically induced contractions in human elbow flexors," *J. Biomech.*, vol. 36, pp. 1713–1718, 2003.

[7] B. Roszek, G. C. Baan, and P. A. Huijing, "Decreasing stimulation frequency-dependent length-force characteristics of rat muscle," *J. Appl. Physiol.*, vol. 77, pp. 2115–2124, 1994.

[8] M. A. Daley and A. A. Biewener, "Muscle force-length dynamics during level versus incline locomotion: a comparison of in vivo performance of two guinea fowl ankle extensors," *J. Exp. Biol.*, vol. 206, pp. 2941–2958, 2003.

[9] F. Sepulveda, D. M. Wells, and C. L. Vaughan, "A neural network representation of electromyography and joint dynamics in human gait," *J. of Biomech.*, vol. 26, pp. 101–109, 1993.

[10] E. A. Clancy, O. Bida, and D. Rancourt, "Influence of advanced electromyogram (emg) amplitude processors on emg-to-torque estimation during constant-posture, force-varying contractions," *Journal of Biomechanics*, vol. 39, pp. 2690–2698, 2006.

[11] K. C. Mountjoy, K. Hashtrudi-Zaad, and E. L. Morin, "Fast orthogonal search method to estimate upper arm hill-based muscle model parameters," in *Proc. 30th International Conference of Engineering in Medicine and Biology Society*, 2008, pp. 3720–3725.

[12] M. J. Korenberg, "A robust orthogonal algorithm for system identification," *Biol. Cybern.*, vol. 60, pp. 267–276, 1989.

[13] F. Mobasser, J. M. Eklund, and K. Hashtrudi-Zaad, "Estimation of elbow-induced wrist force with emg signals using fast orthogonal search," *IEEE Trans. Biomed. Eng.*, vol. 54, pp. 683–693, 2007.

[14] E. E. Cavallaro, J. Rosen, J. C. Perry, and S. Burns, "Real-time myoprocessors for a neural controlled powered exoskeleton arm," *IEEE Trans. Biomed. Eng.*, vol. 53, pp. 2387–2396, 2006.

[15] T. S. Buchanan, D. G. Lloyd, K. Manal, and T. F. Besier, "Neuromusculoskeletal modeling: estimation of muscle forces and joint moment and movements from measurements of neural command," *J. Appl. Biomech.*, vol. 20, pp. 367–395, 2004.

[16] M. A. Lemay and P. E. Crago, "A dynamic model for simulating movements of the elbow, forearm and wrist," *J. Biomech.*, vol. 29, pp. 1319–1330, 1996.